J. Fluid Mech. (2015), *vol.* 772, *pp.* 225–245.
doi:10.1017/jfm.2015.215

Combustion noise is scale-free: transition from scale-free to order at the onset of thermoacoustic instability

Meenatchidevi Murugesan[1,†] **and R. I. Sujith**[1]

[1]Department of Aerospace Engineering, Indian Institute of Technology Madras, Chennai 600036, India

(Received 12 September 2014; revised 1 February 2015; accepted 8 April 2015;
first published online 30 April 2015)

We investigate the scale invariance of combustion noise generated from turbulent reacting flows in a confined environment using complex networks. The time series data of unsteady pressure, which is the indicative of spatiotemporal changes happening in the combustor, is converted into complex networks using the visibility algorithm. We show that the complex networks obtained from the low-amplitude, aperiodic pressure fluctuations during combustion noise have scale-free structure. The power-law distributions of connections in the scale-free network are related to the scale invariance of combustion noise. We also show that the scale-free feature of combustion noise disappears and order emerges in the complex network topology during the transition from combustion noise to combustion instability. The use of complex networks enables us to formalize the identification of the pattern (i.e. scale-free to order) during the transition from combustion noise to thermoacoustic instability as a structural change in topology of the network.

Key words: pattern formation, turbulent reacting flows, wave–turbulence interactions

1. Background

Combustion noise is generated by unsteady combustion processes in propulsion and power-producing systems. Combustion noise is considered as a pollutant. Unlike other chemical pollutants, combustion noise is found to have a direct impact on the listeners (Strahle 1978). Noise can cause physiological changes and even impede the efficiency of the listeners. Exposure of such noise for longer times can even lead to physiological disorders such as hearing loss and interrupted sleep (Dowling & Mahmoudi 2015). Combustion noise is identified to be an important source of noise in industrial furnaces, aero and land-based gas turbine engines. Control of noise emission is of critical importance in view of the increased public concern and increasing stringent regulations.

Combustion noise arises due to the unsteady burning of reacting gases, producing volumetric expansion and compression of fluid near the flame zone. The first explicit analysis of the source of combustion noise was performed by Bragg (1963). He

† Email address for correspondence: mena.murugesan90@gmail.com

modelled the flame as a distribution of monopole sound sources of combustion noise. The flame propagation is described as a locally laminar process and the effect of turbulence is included through the wrinkled flame surface area. However, Bragg's model was based on heuristic arguments and does not rigorously follow the principles of fluid mechanics. A more rigorous analysis was then performed by Strahle (1971) who closely followed Lighthill's theory of aerodynamic noise. An excellent review of the advancements in understanding the sources of combustion noise can be found in Dowling & Mahmoudi (2015).

Spectral analyses of combustion noise generated from open turbulent flames have shown that the acoustic energy spectrum of combustion noise is broadband and involves power-law scaling. Abugov & Obrezkov (1978) showed that the combustion noise spectrum exhibits power-law scaling with a scaling exponent of $-5/2$ in the frequency range of 2–10 kHz. Belliard (1997) also arrived at the power-law scaling with a similar exponent. In the low-frequency range, the acoustic power spectrum is found to have f^{β} dependence and in the intermediate- and high-frequency range, the power spectrum is given by $f^{-\alpha}$ (Rajaram & Lieuwen 2009), where α and β are positive numbers. The power-law scaling ($f^{-\alpha}$) in the high-frequency side of the acoustic power spectrum was shown to have a $P(\omega) \sim \langle |q(\omega)|^2 \rangle$ behaviour, where $P(\omega)$ is the acoustic power and $q(\omega)$ is the heat release rate fluctuations (Rajaram 2007). Clavin & Siggia (1991) and Clavin (2000) related the power law in the acoustic power spectrum of combustion noise to the Kolmogorov spectrum of turbulence. The existence of power laws is an indication of scale invariance that is often seen in physical systems (Lovejoy & Schertzer 1986; Davis *et al.* 1996; Lesne & Laguës 2011).

In practical combustors, flames exist in confined environments. The confinement modes preferentially amplify the sound emitted from the flames at time scales close to their natural time scales (frequencies) and, hence, lead to multiple peaks in the acoustic power spectrum (Chiu & Summerfield 1974; Kumar 1975; Strahle 1978; Hegde, Reuter & Zinn 1988). As a consequence of these peaks in the acoustic power, the scale invariance of combustion noise in a confined environment is hard to discern in the power spectrum.

Further, positive coupling of the heat release rate fluctuations from combustion with the acoustic field in the combustion chamber can lead to large-amplitude pressure oscillations called thermoacoustic instabilities (also known as combustion instabilities) in the community. A review of acoustically coupled combustion-driven oscillations can be found in Dowling & Stow (2003). In addition to acoustics and combustion, vortices that are shed due to hydrodynamics play a key role in driving thermoacoustic instability (Schadow *et al.* 1989; Coats 1996). The vortices shed, grow and impinge at the combustor walls at the instability frequency and the heat release rate fluctuations closely follow the vortex history (Rogers 1956; Yu, Trouve & Daily 1991).

Most of these studies individually investigate and contrast the states of the system during its stable operation (combustion noise) and full-blown combustion instability (Smith & Zukoski 1985; Poinsot *et al.* 1987; Yu *et al.* 1991). However, studies focusing on the transition to combustion instability in a turbulent combustor from a stable regime (combustion noise) in response to the systematic variation of operating conditions of the combustor remain very few in number.

Traditionally, combustion noise and combustion instability are treated as acoustic phenomena driven by combustion. Recently, tools from dynamical systems and complex systems theory are used to understand and quantify the dynamical changes in thermoacoustic systems. Gotoda and co-workers used nonlinear time series analysis

to describe the onset of combustion instability and blowout in a model gas turbine combustor (Gotoda *et al.* 2011, 2012, 2014).

Recently, Nair *et al.* (2013) suggested that the stable regime of a combustor with turbulent flow does not correspond to a fixed point. They suggested that the low-amplitude aperiodic pressure fluctuations during the stable operation of the combustor (known as combustion noise in the community) are deterministic and have chaotic behaviour. During thermoacoustic instability, the acoustic pressure is characterized by large-amplitude, self-sustained, periodic oscillations. In contrast with chaos, these periodic oscillations represent order. The transition from combustion noise to order (i.e. periodic oscillations) happens via intermittency; a state composed of bursts of large-amplitude periodic oscillations, amidst regions of low-amplitude chaotic fluctuations (Nair *et al.* 2013; Nair, Thampi & Sujith 2014).

Currently, we know that transition from combustion noise to combustion instability is associated with change in acoustic amplitude spectrum from one which is broad with shallow peaks to one with sharp peaks at acoustic instability modes (Nair & Sujith 2014; Nair *et al.* 2014). However, there is some vagueness associated with this definition as it is difficult to define what constitutes a shallow peak or a sharp peak. To arrive at a better definition, the pattern emerging during this transition from chaos to order via intermittency needs to be identified and formalized. This involves formalizing the process of pattern discovery (Barabasi 2011).

Further, Nair & Sujith (2014) have shown that combustion noise displays a multifractal signature and this disappears at the onset of thermoacoustic instability. A fractal time series has portions that look similar to the whole time series and have a non-integer dimension. In a multifractal time series, fluctuations of different amplitudes scale differently. Multifractality of combustion noise confirmed the absence of a single characteristic scale in thermoacoustic systems (Nair & Sujith 2014) and reflects the complex nature of the dynamics involved in combustion systems that arises due to the nonlinear interaction between combustion, flow and duct acoustics.

Complexity is a characteristic of real physical systems. Our day-to-day dynamical systems, for example, economic systems, our language or biological systems are ‘complex’ systems, because a great number of interacting elements are involved. The behaviour of a thermoacoustic system, for example, arises from a variety of factors such as molecular mixing, turbulent transport that involves a wide range of scales, chemical kinetics and acoustic wave interaction etc., giving rise to a rich variety of dynamics, giving rise to the possibility of chaotic fluctuations on the one hand to ordered periodic oscillations on the other hand.

Despite the many differences in the nature of complex systems, they often display similar dynamical behaviour. The traditional reductionist approach which attempts to analyse a complex system in terms of its constituent elements, hits its limit in explaining these similarities in fundamentally different physical systems (Barabasi 2011). In this context, a new approach to science has emerged in recent years that investigate how interaction between parts (or elements) gives rise to the collective behaviour of the system. This approach is defined as complex systems approach, where a complex system is reviewed as a system with ‘multiple interacting components whose behaviour cannot be simply inferred from the behaviour of the components’ (http://www.necsi.edu).

Complex network approach represents complex systems as large-scale networks with complex heterogeneous structures and provides a comprehensive understanding of complex connectivity patterns in the dynamical systems. Statistical theory of complex networks is a tool very recently devised to study complex systems (Lesne

& Laguës 2011). The main goal is to formulate quantities to quantitatively describe the topological aspects of the dynamical systems.

Dramatic advances have been made in the past few years in the field of complex networks since the discovery of small-world network by Watts & Strogatz (1998) and scale-free network by Barabási & Albert (1999). Watts & Strogatz (1998) proposed a network model, where starting with a regular topology, with the random addition of few links, the average distance between nodes reduced drastically. Such a network is known as small-world network. The small-world network model is successful in describing the transition from regular to random topology, popularly known as the Watts and Strogatz (WS) model. Both small-world and random networks follow exponential distribution of connectivity in the network. Later, in 1999, Barabási & Albert (1999) discovered that most of the real-world networks such as the Internet, World Wide Web and scientific collaboration networks have a heavy-tailed distribution of connectivity with no characteristic scale; such networks are called 'scale-free' networks. Surprisingly, despite their differences, most of the complex systems such as biological systems (Alm & Arkin 2003; Barabasi & Oltvai 2004), World Wide Web (Barabasi, Albert & Jeong 1999; Albert, Jeong & Barabasi 2000) and power grids (Arianos *et al.* 2009; Chen *et al.* 2010; Pagani & Aiello 2014) possess scale-free topological structure.

Time series data are the reflection of the underlying spatiotemporal dynamics of any system. For example, the time series data of fluctuating quantities measured in the flow are shown to have direct correlation with the features of flow patterns in two-phase flows (Rouhani & Sohal 1983; Das & Pattanayak 1993). In nonlinear sciences, complex networks are used to understand the dynamics underpinning the time series data (Zhang & Small 2006; Lacasa *et al.* 2008; Donner *et al.* 2010). A general framework has been developed to transform time series into complex networks and vice versa (Strozzi *et al.* 2009). This dual vision enables us to visualize the information hidden in the dynamics of a time series as different structures in the corresponding complex networks.

It has been recently demonstrated that complex networks can be used to distinguish the flow patterns in gas–liquid two phase flows (Gao & Jin 2009; Gao *et al.* 2010) and various regimes of turbulent jet flows (Charakopoulos *et al.* 2014). Detecting the patterns or structures in the complex network obtained from a thermoacoustic system may enable us to obtain an alternative definition and characterization of thermoacoustic transition. In the present paper, we make a first attempt to investigate signals generated by the interaction between acoustics, combustion and turbulence from the complex networks perspective, with the hope that tools from the field of complex networks can stimulate the study of combustion dynamics from an alternative perspective.

We derive complex networks from the time series data of dynamic pressure measured at different operating conditions in a combustor. We show that low-amplitude, aperiodic pressure fluctuations during combustion noise in a confined environment can be represented as a scale-free network. Scale-free network manifests the scale invariance of combustion noise and implies that there is no single characteristic scale in the network. A scale-free network follows a power-law behaviour between $P(k)$ and k (i.e. $P(k) \sim k^{-\gamma}$, where γ is a positive number), where k is the number of nodes connected with a given node and $P(k)$ is the percentage of nodes with k number of connections in a given network (Barabasi & Bonabeau 2003). This power-law distribution of the scale-free network is related to the scale invariance of combustion noise.

There is a loss of scale invariance at the onset of thermoacoustic instability, i.e. the scale-free behaviour transitions to an orderly behaviour (periodic oscillations). We show that the time series data acquired during instability (periodic oscillations) can be represented as a regular network that has ordered topological features. In the transition to thermoacoustic instability, the appearance of intermittent bursts of periodic oscillations changes the topology of the complex network. We illustrate the transition from a scale-free structure to an ordered regular structure in the topology of the complex networks during the transition from combustion noise to thermoacoustic instability.

The rest of the paper is organized as follows. Complex networks and methods to extract complex networks from time series are briefly described in § 2. The details of the experiments are provided in § 3. Representation of time series as complex networks and the topological change from scale-free to regular during the transition from combustion noise to thermoacoustic instability along with its physical interpretation are discussed in § 4. The key results are summarized in § 5.

2. Extracting complex networks from the time series data

A complex network consists of nodes and connections between the nodes. Many different methods can be used to construct a complex network from a time series. As an example, conditions based on temporal correlation of pseudo-periodic cycles (Zhang & Small 2006), recurrence of states in phase space (Donner *et al.* 2010), visibility of nodes (Lacasa *et al.* 2008) are used to connect the nodes in a network. We use the visibility graph (Lacasa *et al.* 2008) to represent a thermoacoustic system as a complex network. We then show the topological changes in complex networks during the transition from combustion noise to thermoacoustic instability via intermittency.

From the acquired data, we construct a new time series by considering only the peaks in the time series data. The data points in the new time series are represented as vertical bars. As an example, let $x(t)$ be the acoustic pressure time series and $\boldsymbol{p}(t)$ be the vector that consists of data points belonging to the crest of each cycle in the time series. Each data point in the vector $\boldsymbol{p}(t)$ is considered as a node. Information about the connectivity between nodes is stored in an adjacency matrix (Donner *et al.* 2010). As an example, if two nodes i and j are connected, $A_{i,j}$ is one; otherwise $A_{i,j}$ is zero. To avoid self-connections, $A_{i,i}$ is chosen as 0 in the adjacency matrix.

2.1. *Visibility graph*

According to the visibility condition, each data bar or data value in the time series $\boldsymbol{p}(t)$ is considered as a node (Lacasa *et al.* 2008). Any two nodes are connected when a straight line can be drawn between these two nodes without intersecting any intermediate data bars. The method is illustrated in figure 1.

Two nodes (i and j) are connected if the intermediate nodes ($i < k < j$) satisfy the following condition,

$$A_{i,j} = \begin{cases} 1, & \text{if, } \; p_k < p_i + (p_j - p_i)\dfrac{t_k - t_i}{t_j - t_i}, \\ 0, & \text{otherwise.} \end{cases} \tag{2.1}$$

The method discussed above is employed to extract a complex network from the time series data of unsteady pressure measured from a combustor described in the following section.

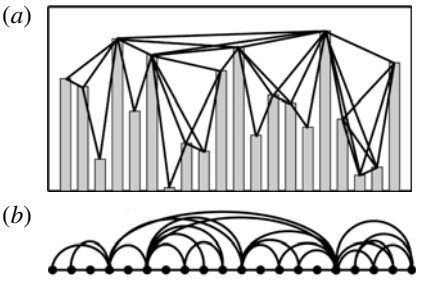

FIGURE 1. Illustration of visibility graph to convert a time series into a complex network. (*a*) The time series to be converted into a complex network is represented as vertical bars. Each data point in the time series $\boldsymbol{p}(t)$ is converted into a node appearing as a black dot in figure 1(*b*). If a straight line can be drawn between any two nodes (i.e. data heights i and j) without intersecting any nodes ($i < k < j$) between them, nodes i and j are connected. If two nodes are connected, a connection is drawn between them in the network as shown in figure 1(*b*). (*b*) The complex network with nodes and connections derived from the time series shown in figure 1(*a*), using the visibility condition.

3. Experiments

The experimental configurations and the unsteady pressure data presented in the current work is the same as that described in Nair & Sujith (2014) and Nair *et al.* (2014). These experiments were performed in a combustor with two different flame holding mechanisms: a vane swirler and a circular bluff body, in a turbulent environment ($Re > 16\,000$). The set-up consists of a settling chamber, burner and combustion chamber with extension ducts. The combustion chamber is 700 mm long with a square cross-section (90 mm × 90 mm). The bluff body is a circular disk of 47 mm diameter and 10 mm thickness, supported by a central shaft of 16 mm diameter. For the experiments with swirler as a flame holding device, the bluff body was replaced with swirler. The swirler composed of eight blades with a vane angle of 40°. The position of the flame holding device (both swirler and bluff body) can be varied inside the combustion chamber using a rack and pinion mechanism. Liquefied petroleum gas (LPG; composed of 60 % of C_4H_{10} and 40 % of C_3H_8 by volume) is used as the fuel. The fuel is supplied into the chamber through a central shaft and injected 160 mm before the rear end of the bluff body through four radial injection holes of diameter 1.7 mm. Air is supplied from a high-pressure chamber through a moisture filter to the settling chamber. The flow rates of fuel and air are measured using mass flow controllers (Alicat Scientific, MCR series) in terms of standard litres per minute (SLPM standardized for air at temperature of 25 °C and pressure of 143 696 psi with an uncertainty of ±0.8 % of reading +2 % of full scale). The acoustic pressure data presented in this paper is measured at 90 mm from the upstream end of the combustion chamber using a piezoelectric transducer with a sensitivity of 72.5 mV kPa^{-1} and uncertainty of ±0.64 %. The schematic of the set-up and further details on experimentation can be found in Nair & Sujith (2014) and Nair *et al.* (2014).

4. Results and discussions

The acoustic pressure measurements during the occurrence of combustion noise acquired from turbulent combustor with (*a*) a circular bluff body and (*b*) a swirler

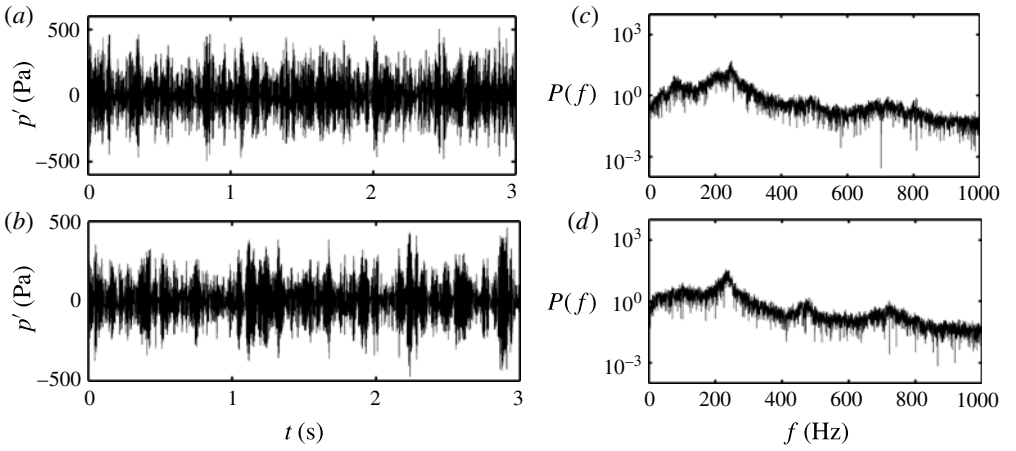

FIGURE 2. Acoustic pressure time series data acquired during combustion noise in a combustor with (*a*) bluff body ($Re = 1.8 \times 10^4$) and (*b*) swirler ($Re = 1.6 \times 10^4$) as flame holding device. The unsteady pressure exhibits low-amplitude, seemingly random, irregular fluctuations. The amplitude spectrum of combustion noise from (*c*) bluff-body stabilized configuration and (*d*) swirler stabilized configuration. The amplitude spectra of acoustic pressure are broadband with shallow peaks in the vicinity of the acoustic modes of the combustor.

as flame holding device are shown in figure 2(*a*,*b*). The acoustic pressure exhibits low-amplitude, seemingly random, irregular fluctuations. The corresponding acoustic pressure amplitude spectra (figure 2*c*,*d*) are broadband with shallow peaks near the acoustic modes of the combustor.

Assuming linear acoustics, the sound emission at each frequency from open turbulent flames is shown to be generated from heat release process at that frequency (Rajaram 2007). When such turbulent flames are confined in a combustion chamber, the confinement modes preferentially amplify the sound emitted from the flames at time scales close to their natural time scales (frequencies) and gives rise to the shallow peaks in the amplitude spectrum. The presence of multiple peaks in acoustic power spectrum during combustion inside a confinement is reported in literature (Chiu & Summerfield 1974; Kumar 1975; Strahle 1978; Hegde *et al.* 1988). However, combustion chamber acoustics and hydrodynamics do not lock on during combustion noise and, hence, do not lead to the excitation of self sustained combustion instabilities (Chakravarthy *et al.* 2007*a*; Chakravarthy, Sivakumar & Shreenivasan 2007*b*).

As we have already mentioned in § 1, the acoustic power spectrum of combustion noise from open turbulent flames involves a power-law scaling. The physical reason for the power-law scaling in the acoustic power spectrum in combustion noise is turbulence. Clavin & Siggia (1991) and Clavin (2000) showed that if the turbulence have Kolmogorov spectrum, the acoustic power spectrum varies as $\omega^{-5/2}$. Power laws are an indication of scale invariance often seen in physical systems (Lovejoy & Schertzer 1986; Davis *et al.* 1996; Lesne & Laguës 2011).

Scale invariance is an important feature of turbulent flows (Pocheau 1994; Frisch 1995; Lesne & Laguës 2011). However, such power-law scaling is not discernable in the amplitude spectrum for combustion noise in a confined environment (see figure 2*c*,*d*) due to the presence of narrow peaks near the duct modes. To unveil

the scale invariance of combustion noise in a confined environment, we employ the statistical theory of complex networks.

4.1. *Complex network representation of combustion noise*

The time series data of acoustic pressure representing the dynamics of combustion noise is mapped into complex networks using visibility algorithm which is explained in § 2. If any two nodes (i and j) are connected $A_{i,j}$ is one, otherwise $A_{i,j}$ is zero. Any node ($i = 1, \ldots, N$, N is the total number of nodes in the network) can be connected to a number of other nodes ($j = 1, \ldots, N-1$) present in the network. The total number of nodes that are connected with a given node v is specified as the degree of that node ($k_v = \sum_{i=1}^{N} A_{i,v}$). The percentage of nodes with k number of connections in a complex network can be represented using a distribution $P(k)$. The variation of $P(k)$ with respect to k is important in distinguishing the different types of complex networks. As an example, if the variation of $P(k)$ with respect to k follows a random distribution (Poisson distribution, exponential distribution, etc.), the corresponding network is classified as a random network (Zhang & Small 2006).

The degree distribution of complex networks mapped from the unsteady pressure time series during combustion noise acquired from (a) bluff-body configuration and (b) swirler configuration are shown in figure 3(a,b).

As can be seen from figure 3(a,b), the degree distribution of complex networks mapped from time series data during combustion noise has a power-law behaviour:

$$P(k) \sim k^{-\gamma}. \tag{4.1}$$

The power law exponents are measured to be $\gamma = 2.7$ for bluff-body configuration and $\gamma = 2.5$ for swirler configuration with an uncertainty of ± 0.1. For all of the data that we obtained in the bluff-body or swirler configurations, the power law exponent of scale-free network during combustion noise was in the range of 2.5–2.7. This highlights the fact that the power-law exponents ($\gamma = 2.7$ and 2.5) are nearly identical for two different (bluff-body and swirler) configurations.

From the power law trend, we discover that the complex networks obtained during combustion noise are scale-free networks. This is the first time in thermoacoustics literature that time series data acquired during combustion noise is represented as scale-free network. Time series obtained from turbulent systems have been recently represented as scale-free networks (Liu, Zhou & Yuan 2010; Charakopoulos *et al.* 2014).

Scale-free behaviour of complex network corresponding to combustion noise represents the scale invariance of combustion noise. The power law distributions of scale-free network are related to the fractality (scale invariance) of the original time series (Zhang & Small 2006; Lacasa *et al.* 2008). For non-stationary time series, Lacasa *et al.* (2009) proposed a linear correlation between the power-law exponent and the Hurst exponent. In statistical analysis, non-stationary time series is the one for which statistical properties (for example mean, variance, central moments, etc.) does not remain constant in time. The acoustic pressure time series data acquired during combustion noise is non-stationary since pressure measurements acquired at a given instant is not only a function of the previous instant, but also depends on the changes happening at some other locations in the reacting flow. If we crudely apply the equation relating Hurst exponent and power-law exponent ($\gamma = 3.1 - 2H$) given by Lacasa *et al.* (2009) and Ni, Jiang & Zhou (2009), we get Hurst exponent of $H = 0.2$ for bluff-body configuration and $H = 0.3$ for swirler configuration.

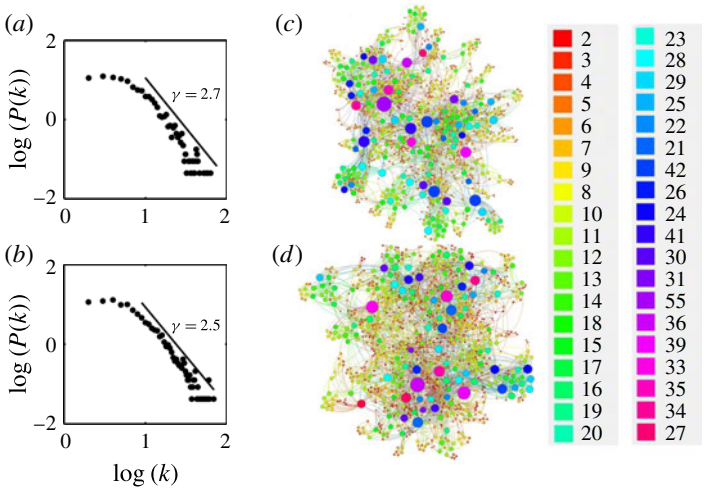

FIGURE 3. (*a*) Degree distributions ($P(k)$ versus k) of the complex network during combustion noise acquired from (*a*) bluff-body configuration ($Re = 1.8 \times 10^4$) and (*b*) swirler configuration ($Re = 1.6 \times 10^4$). It is evident from figure 3(*a*,*b*), that the degree distribution curve has a power-law behaviour highlighting that networks during combustion noise are scale-free. The physical mechanism underlying scale-free nature (scale invariance) of combustion noise is the turbulence involving vortices that span a range of scales in the inertial regime. Complex networks during combustion noise acquired from (*c*) bluff-body configuration and (*d*) swirler configuration are plotted using the Gephi software. Nodes are shown as circles and coloured based on their degree (degree of a node is the number of nodes connected with that node). The sizes for nodes are assigned based on their degree. A few large nodes that are connected with highest number of nodes (called hubs) in a network correspond to a few large vortices in the flow. It can be seen that blue and pink coloured nodes are connected with largest number of nodes and are the hubs in a scale-free network of combustion noise. Nodes with fewer degrees are due to the intermediate and small-scale vortices in the flow. The complex network during combustion noise possesses heterogeneity of degrees of nodes with no characteristic degree.

The value of the Hurst exponent ($0 < H = 0.2, 0.3 < 0.5$) implies that combustion noise data is antipersistent. For antipersistent time series, a large data value is followed by a small value and a small value is followed by a large value. For antipersistent signals, the value of Hurst exponent lie between 0 and 0.5. These results on Hurst exponent are consistent with the results reported by Nair & Sujith (2014).

The networks derived during the occurrence of combustion noise are plotted (figure 3*c*,*d*) using the Gephi software (Bastian, Heymann & Jacomy 2009). The nodes are shown as circles. Nodes of different degrees are shown in different colours (degree of a node is the number of nodes connected with that node). Further, nodes are shown in different sizes based on their degree. As can be seen from figure 3(*c*,*d*), the complex networks during combustion noise possess heterogeneity of degrees of nodes. There is no characteristic degree in this network which is the reason why they are scale-free networks.

The heterogeneity in degrees of nodes can be directly linked to the physical state of combustion noise. Turbulent reacting flows involve scales that span a range from large scales of the order of the characteristic dimension of the flow to Kolmogorov scales. A few large vortices in the reacting flows produce fluctuations of large magnitudes

which are reflected as large fluctuations of data values in the time series. As we move towards the intermediate and small vortices, the number of small-scale, short-living vortices increases. These high-frequency small eddies in the reacting flows produce fluctuations of small magnitude which result in small fluctuations of data values in the time series. Nodes that correspond to larger data values in the time series have visibility to many other nodes that correspond to small data values in the time series. Therefore, nodes with large data values are connected with more number of other nodes in a network. Such nodes that are connected directly with a very large number of other nodes in a network are called hubs.

Hubs are the key nodes in the network and only a few such hubs can be found in a network. These hubs are the reflection of large-scale vortices in the turbulent flow. In the degree distribution, nodes with the highest degree occur in minimum percentage to the total number of nodes (occupies the tail portion of the power-law curve). As an example, in a scale-free network of combustion noise (figure 3*c*), a few hubs (nodes that are coloured in blue and pink) connected with a large number of other nodes can be seen.

In contrast, nodes having small data values can see only a few of their neighbours and are connected with only a few other nodes. These nodes with lower degrees occur as large population and are a reflection of short-living, large number of small-scale eddies in the flow. In the degree distribution, we can see a higher percentage of nodes having fewer degrees. In complex networks (figure 3*c*), these nodes can be seen as a large number of small size nodes with fewer connections.

The cascade of vortices of different scales leads to the absence of a single characteristic scale and is the physical reason for the scale-free behaviour of combustion noise. The scale invariance (i.e. power-law distribution) of combustion noise in a confined environment is unraveled in the complex network representation as scale-free behaviour, although such scale invariance cannot be discerned in the amplitude spectrum.

4.2. *Combustion noise to combustion instability: transition from scale-free to regular network*

The scale-free behaviour of combustion noise gives a hint that the addition of heat in turbulent flows (corresponding to the case of combustion in turbulent flows) preserves the scale invariance which is in fact a property of turbulent flows. However, the transition to the onset of combustion instability from combustion noise is associated with the change in system dynamics from one dominated by the presence of multiple scales to one dominated by a few discrete scales. The transition in system dynamics during this transition (combustion noise to combustion instability) for increasing flow Reynolds number in a bluff-body stabilized turbulent combustor is illustrated in terms of changes in the time series data of acoustic pressure (figure 4).

As we have already discussed in § 4.1, the acoustic pressure measured during combustion noise is characterized by aperiodic fluctuations (figure 4*a*). However, as we increase the Reynolds number further past the condition of combustion noise, ordered periodic oscillations appear intermittently amidst regimes of aperiodic fluctuations.

This intermediate state characterized by alternating appearances of bursts of periodic and chaotic fluctuations is identified to be ‘intermittency’ (shown in figure 4*b*,*c*) (Nair *et al.* 2014). Such an intermittent state is a dynamical state different from combustion noise and combustion instability and is observed consistently every time during the

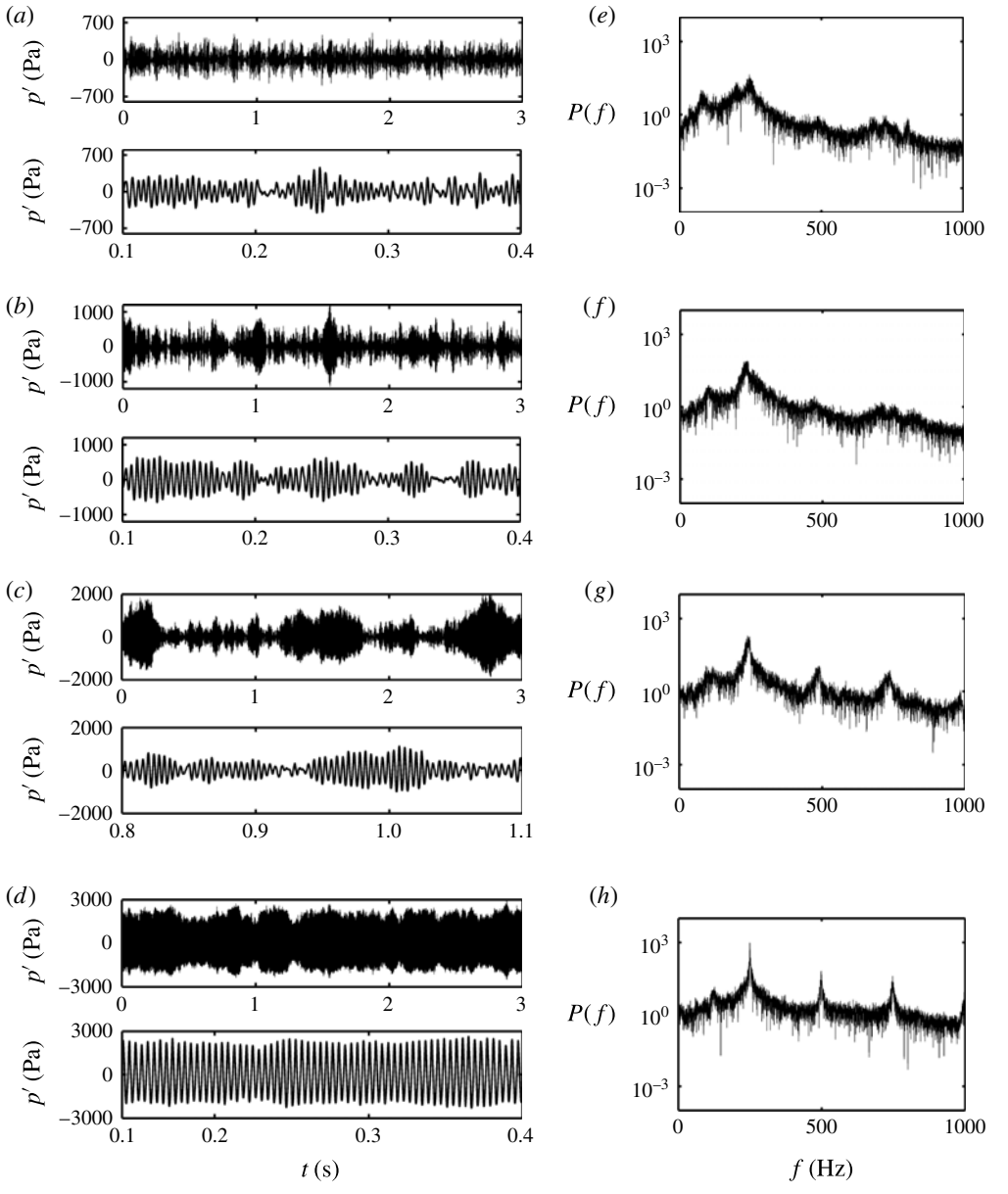

FIGURE 4. As the Reynolds number is increased further past the condition of combustion noise, intermittency is observed. Unsteady pressure time series measured in bluff-body configuration during (*a*) combustion noise ($Re = 1.7 \times 10^4$), intermittency when (*b*) $Re = 2.2 \times 10^4$ and (*c*) $Re = 2.5 \times 10^4$. Intermittent bursts of high-amplitude periodic oscillations amidst regimes of chaotic fluctuations last longer in time as we increase the Reynolds number towards the condition of combustion instability. Finally, when (*d*) $Re = 2.8 \times 10^4$, self-sustained, high-amplitude, ordered periodic oscillations happen during full-blown combustion instability. Transition from combustion noise to combustion instability is reflected as a transition from chaos to limit cycle in the time series of acoustic pressure. The accumulation of acoustic energy, reflected as growth in acoustic pressure amplitude in the amplitude spectrum in the vicinity of acoustic instability modes, is observed during this transition to combustion instability.

transition from combustion noise to combustion instability and persists in time. Intermittency is not a transient state, but a distinct state described by dynamical systems theory.

From a dynamical systems perspective, intermittency is explained as a result of homoclinic orbits in the phase space by Nair & Sujith (2013). A homoclinic orbit is a trajectory in phase space in which an unstable manifold of a fixed point of the system merges with its own stable manifold (Nair & Sujith 2013). The equilibrium state of the system during intermittency switches between stable and unstable states in phase space. This corresponds to the alternate switching of bursts of high-amplitude periodic oscillations and low-amplitude chaotic fluctuations in the unsteady pressure time series data (see figure 4*b*,*c*).

These intermittent bursts of high-amplitude periodic oscillations last longer in time as we increase the Reynolds number towards the condition of combustion instability. Finally, self-sustained, high-amplitude, ordered periodic oscillations happen during full-blown combustion instability (figure 4*d*). Therefore, the transition from combustion noise to combustion instability is reflected as a transition from chaos to limit cycle (order) in the time series of acoustic pressure.

Complex networks are constructed from the time series data of acoustic pressure acquired during this transition. The degree distributions of the complex networks during intermittency (shown in figure 5*a*,*b*) have a power-law behaviour. This shows that time series acquired during intermittency are also converted into scale-free networks. The scale-free networks during intermittency are plotted with the help of the Gephi software (Bastian *et al.* 2009) and as one would expect, these networks also has no characteristic degree (figure 5*d*,*e*).

In contrast to intermittency and combustion noise, complex networks during limit cycle oscillations (figure 5*f*) exhibit increased regularity in the degrees of the nodes. As can be seen in figure 5(*c*), the degree distribution map is characterized by a few discrete points. The slight non-uniformity in degrees of the nodes (figure 5*f*) is due to the cycle-to-cycle variability in limit cycle oscillations (see figure 4*d*) during combustion instability which arises from background turbulent fluctuations (Lieuwen 2002). Through extensive investigation, Lieuwen (2002) showed that such cyclic variability does not reflect the presence of chaotic fluctuations. Rather, Lieuwen (2002) suggested that the cyclic variability in limit cycle oscillations arise from background disturbances with short correlation time relative to the period of limit cycle. The imperfect limit cycle oscillations in the dynamics of turbulent combustors are also reported and characterized by Noiray & Schuermans (2012).

To visualize results in a better manner in such 'noisy' situations, Nunez *et al.* (2012) introduced a threshold 'epsilon' to visibility condition.

$$A_{i,j} = \begin{cases} 1, & \text{if, } p_k + \varepsilon < p_i + (p_j - p_i)\dfrac{t_k - t_i}{t_j - t_i}, \\ 0, & \text{otherwise,} \quad \text{where, } \varepsilon = e \times \text{mean}(\boldsymbol{p}). \end{cases} \tag{4.2}$$

Here, $\boldsymbol{p}$ is the vector that consists of data values belonging to the crest of each cycle in the time series. The time series data of acoustic pressure acquired from the combustor possess fluctuations of different scales. This causes, peaks (i.e. crest of each cycle in the time series) in the acoustic pressure time series to have both positive and negative values varying in a wide range. As an example, for time series data during combustion noise (when $Re = 1.8 \times 10^4$), the maximum value of the peaks

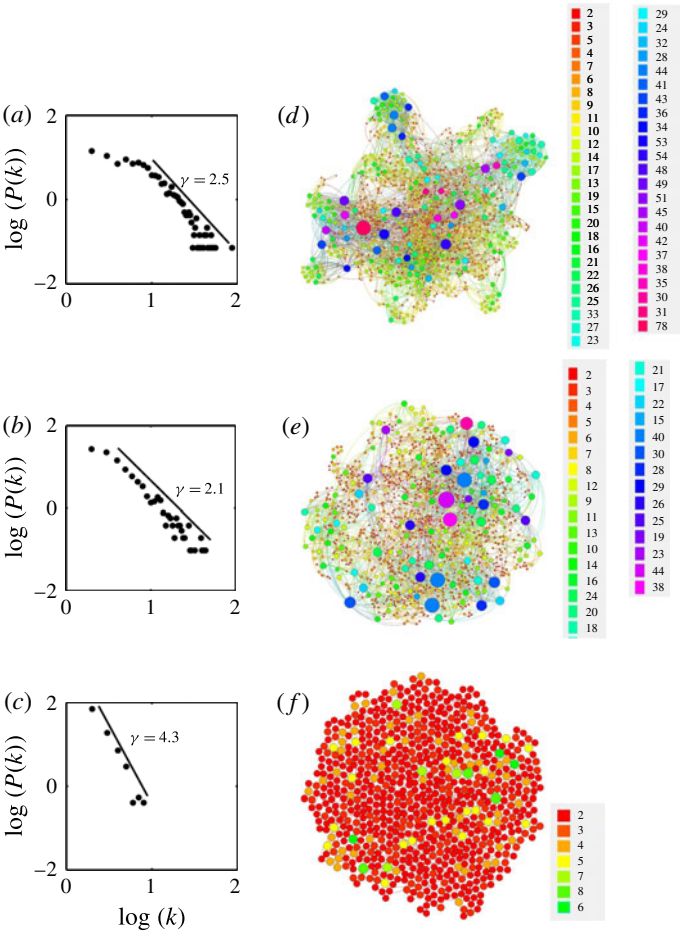

FIGURE 5. Degree distributions of complex networks derived using visibility condition from time series of acoustic pressure during intermittency (shown in figure 4*a*,*b*) when (*a*) $Re = 2.2 \times 10^4$ and (*b*) $Re = 2.5 \times 10^4$. The degree distribution curves have power-law trend showing that time series during intermittency are also converted into scale-free networks. The networks are plotted with the help of the Gephi software (Bastian *et al.* 2009). As one would expect, networks during intermittency (*d*,*e*) also have no characteristic degree. In contrast, (*f*) network during combustion instability when $Re = 2.8 \times 10^4$, possess increased regularity in degrees of nodes. However, turbulence causes imperfection in periodicity. (*c*) The degree distribution map during instability is characterized by a few discrete points.

is 516.5 Pa, the minimum value of the peaks is −441.4 Pa and the mean value of the peaks is 58.3 Pa. Therefore, the threshold $\varepsilon = 0.24 \times \text{mean}(\boldsymbol{p})$ is 13.992 Pa which is 2.7 % of maximum value of the peaks. Since the value of ε is very small with respect to the peak amplitude; we consider that the information in the time series is preserved with the addition of epsilon into the visibility algorithm.

The degree distributions of complex networks during (*a*) combustion noise, (*b*) intermittency and (*c*) combustion instability with the use of epsilon in the visibility graph are shown in figure 6.

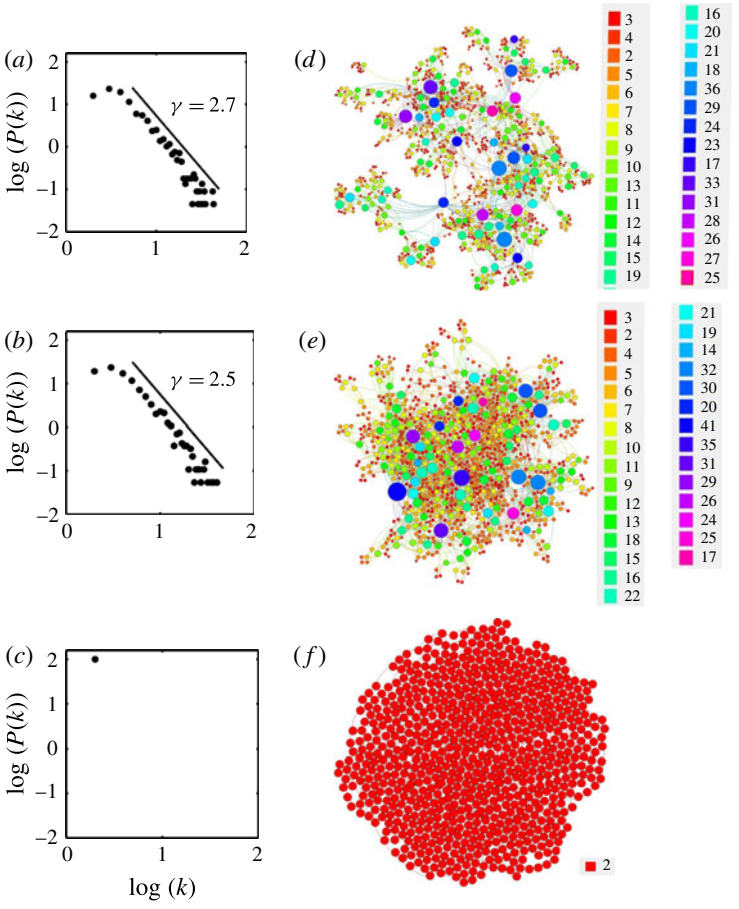

FIGURE 6. Degree distributions and networks derived using visibility graph with threshold ($e = 0.24$) during the occurrence of (*a*) and (*d*) combustion noise ($Re = 1.8 \times 10^4$), (*b*) and (*e*) intermittency ($Re = 2.2 \times 10^4$) and (*c*) and (*f*) combustion instability ($Re = 2.8 \times 10^4$). The power-law exponent of degree distributions during the occurrence of (*a*) combustion noise and (*b*) intermittency remains the same as that of networks without using a threshold. The use of ε in the visibility condition helped in detecting the periodicity hidden in the noisy limit cycle oscillations during combustion instability. At the onset of combustion instability, the scale-free behaviour disappears and the network transitions into a regular network. The regular network corresponding to the combustion instability is characterized by a single characteristic degree. All of the nodes have the same number of links with other nodes in the network and a discrete point appears in the plot of $P(k)$ versus k (*c*).

The degree distributions of complex networks derived using the visibility condition with ε during the occurrence of combustion noise (figure 6*a*) and intermittency (figure 6*b*) remain qualitatively same as that of degree distributions of complex networks derived without using ε in visibility condition during combustion noise (figure 3*a*) and intermittency (figure 5*a*). The power-law exponents of complex networks during combustion noise and intermittency do not change with the inclusion of ε into the visibility condition, implying that the corresponding networks are indeed scale-free (the degree distributions of complex networks for different values of

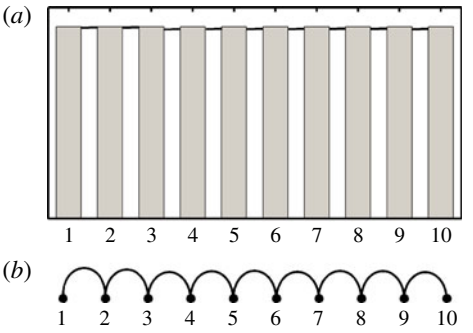

FIGURE 7. Illustration of complex network derived using visibility graph from a periodic time series. Peaks in the periodic time series are considered as nodes. All of the nodes are of the same height and have visibility only with their neighbours. Therefore, all of the nodes are connected only with their neighbours.

threshold are provided in appendix A). However, the main advantage of incorporating ε into the visibility algorithm is the detection of periodicity in the time series which is masked by the presence of irregular fluctuations in experiments.

In contrast to combustion noise and intermittency, degree distribution of complex network during combustion instability is characterized by a single discrete point (figure 6*c*). Discrete points appear in the degree distribution of a regular network. A network is called 'regular' if all of the nodes in the network have the same number of connections (Quenell 1994). The period-one time series (limit cycle) is converted into a regular network with a single point in the degree distribution map (Quenell 1994). The situation is illustrated using figure 7.

In an example illustrated in figure 7, nodes are connected only with two of their neighbours. Therefore, the degree (number of nodes that are connected with a given node) of all of the nodes become two. During the occurrence of combustion instability, all of the nodes are connected only to their neighbours. Thus, in the degree distribution (figure 6*c*) of a complex network that correspond to combustion instability, the percentage of nodes ($P(k)$) having degree $k = 2$ is 100 %, implying that the network at combustion instability is 'regular'.

The complex networks during (*d*) combustion noise, (*e*) intermittency and (*f*) combustion instability with the use of epsilon in the visibility graph are shown in figure 6. Nodes of different degrees are shown in different colours. The colour code with respect to degree is provided near the corresponding complex networks in figure 6. Further, sizes for nodes are assigned based on their degree.

The network of combustion noise and intermittency are composed of nodes of various degrees and various sizes. Nodes are filled with various colours and the network has no single characteristic degree. At combustion instability, all of the nodes in the complex network have a degree of two due to the periodic oscillations and hence the entire network is coloured in red.

The transition from combustion noise to combustion instability is shown as transition from scale-free to regularity in complex networks topology. The physical mechanism underlying this transition is linked with the mechanisms that cause order to emerge in turbulent systems.

In the transition from turbulence to order, fully developed turbulent flow is shown to be self-organizing into an ordered state through the mechanism of spectral

condensation and inverse energy cascade (Shats, Xia & Punzmann 2005). The turbulent energy in a broadband spectrum is redistributed to form an ordered state at high energy level (Kraichnan 1967; Dubos *et al.* 2001; Shats *et al.* 2005). In this spectral redistribution, the turbulent energy is shown to be accumulated in the lowest accessible mode (Sommeria 1986; Paret & Tabeling 1998; Shats *et al.* 2005). In thermoacoustic systems, during the transition to thermoacoustic instability from combustion noise, the growth in the acoustic pressure amplitude close to the acoustic modes of the combustor can be seen in the acoustic amplitude spectrum (figure 4*f–h*). Finally, at full blown combustion instability the acoustic pressure amplitude reaches a maximum value near the duct acoustic modes. Moreover, it is well known in the literature that combustion instability is associated with the formation of organized coherent vortices in the flow indicating an increase in order of the thermoacoustic system (Smith & Zukoski 1985; Poinsot *et al.* 1987; Yu *et al.* 1991). Hence, we conjecture that the transition from combustion noise to combustion instability may be due to the self-organization of multiple scales in turbulence to an ordered state with a single scale.

Further, self-organization of turbulent fluids to a high-energy ordered state is identified to be due to the mechanism of inverse energy cascade (Sommeria 1986; Paret & Tabeling 1998; Dubos *et al.* 2001; Shats *et al.* 2005; Xiao *et al.* 2009). However, this inverse energy cascading is in contrast to conventional paradigm of energy being transferred from large to smaller scales until the scales of dissipation. Inverse energy cascade was first conjectured by Kraichnan (1967) who proposed that energy in a forced turbulent fluid can cascade to larger scales. In turbulent reacting flows, heat release rate fluctuations from combustion supply energy into acoustics. The interaction of the generated acoustic waves with shear layer induces the formation of vortices of different sizes. The size of vortices depends on the hydrodynamic instability frequency matching with the acoustic instability frequency (Schadow & Gutmark 1992). The occurrence of large-amplitude pressure fluctuations during combustion instability is driven by periodic heat release rate fluctuations, when heat release rate fluctuations are in phase with acoustic pressure fluctuations. This is a necessary condition known as Rayleigh criterion (Rayleigh 1878) for self-sustained pressure oscillations. Therefore, the process of combustion instability could possibly be expected to be driven by the inverse cascading of energy from combustion to large scales which are in turn decided by the matching of hydrodynamic frequency and acoustic mode. This is in agreement with the observation of the development of large-scale vortices driving combustion instability (Rogers 1956; Smith & Zukoski 1985; Poinsot *et al.* 1987; Schadow *et al.* 1989; Yu *et al.* 1991; Coats 1996). Further, Zank & Matthaeus (1990) indicated the possibility of inverse energy cascade, wherein energy is cascaded to long-wavelength acoustic modes from smaller scales in the theoretical analysis of nearly incompressible flows with heat addition.

From a complex networks perspective, with a single scalar pressure measurement, the patterns emerging during this transition are visualized as the structural changes happening in the topology of complex networks. Further, these structural changes can be quantified in terms of network properties. The network properties are used to distinguish different dynamical regimes in turbulent jet flows (Charakopoulos *et al.* 2014) and three-dimensional fully developed turbulence (Liu *et al.* 2010). We have utilized the properties of complex networks to provide early warning for the onset of instabilities in many types of combustors and an aeroacoustic system operated in a turbulent environment (Murugesan, Nair & Sujith 2014).

5. Conclusions

We investigated the scale invariance of combustion noise generated from confined turbulent flames using complex networks. We showed that acoustic pressure fluctuations, which reflect the dynamics of combustion noise, can be represented as a scale-free network. The power law exponent in the degree distribution of scale-free network is related to the scale invariance of combustion noise. Scale-free network indicates that there is no single characteristic scale in the dynamics of combustion noise. This scale-free behaviour of combustion noise is hard to discern from the frequency spectrum, due to the domination of duct acoustic modes. The scale-free behaviour of combustion noise is due to the presence of turbulence. The spatial/temporal fluctuations that range from large scales of the order of characteristic dimension of the flow to small Kolmogorov scales in turbulent reacting flows give rise to the complex topology and heterogeneous structure in network during combustion noise.

This scale-free network is shown to transition into regular network during the transition from combustion noise to combustion instability. The presence of scale-free behaviour in combustion noise and the emergence of order from scale-freeness at the onset of combustion instability draw attention to the possibility of spectral condensation and inverse energy cascade which can possibly explain the emergence of order. Complex network representation helped visualize and formulate quantities to quantitatively describe the topological changes during this transition. The variation of network properties can be used to provide early warning for the onset of combustion instability. Further research on self-organization or self-evolution of complex networks can help in developing a complex network model for thermoacoustic systems and explore the underpinning mechanisms.

Acknowledgements

The authors would like to thank Dr V. Nair and Mr V. R. Unni for providing the data presented in this paper. The authors would like to thank Mr E. A. Gopalakrishnan for his valuable suggestions regarding the implementation of the complex network approach to thermoacoustics.

Appendix A. Visibility algorithm with ε to investigate transition from combustion noise to combustion instability

The degree distribution maps of complex networks derived during combustion noise (figure 8*a*), intermittency (figure 8*b*) and combustion instability (figure 8*c*) using different values of ε are shown in figure 8.

The power-law behaviour of networks during the occurrence of combustion noise (figure 8*a*) and intermittency (figure 8*b*) remains the same and power-law exponents do not change for different values of ε considered in the present work. This shows that combustion noise and intermittency remain scale-free with the use of ε. However, for increasing values of e from 0.1 to 0.24 (results are presented for values of $e = 0.1$, 0.15, 0.2 and 0.24 in figure 8), number of points in the degree distribution map of complex network that correspond to combustion instability decreases along with an exponential increase in the value of power-law exponent. For all $e \geqslant 0.24$, the network during combustion instability possesses a discrete point in the degree distribution map. Figure 8 confirms that use of epsilon helps in detecting the periodicity hidden in limit cycle oscillation during combustion instability and does not filter the information in the time series.

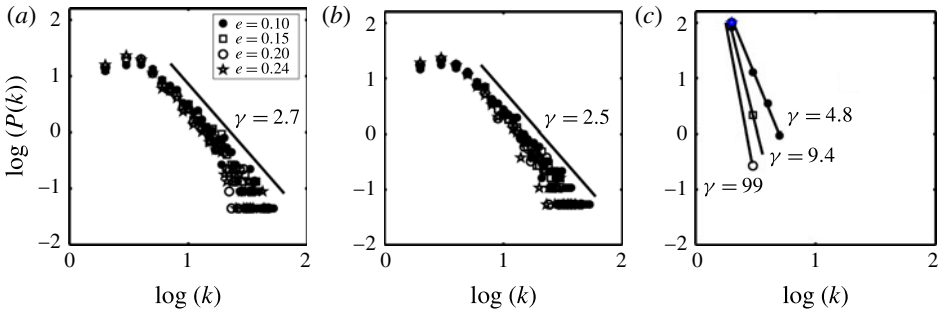

FIGURE 8. (Colour online) Degree distribution maps of networks constructed from time series data of (*a*) combustion noise ($Re = 1.8 \times 10^4$), (*b*) Intermittency ($Re = 2.2 \times 10^4$) and (*c*) combustion instability ($Re = 2.8 \times 10^4$) for different values of e. For all e, combustion noise and intermittency remain to be scale-free. Use of ε helps us to detect periodicity in time series data during combustion instability. For all $e \geqslant 0.24$, network during combustion instability possess a discrete point in the degree distribution map, indicating that corresponding network is regular. The transition from combustion noise to combustion instability is reflected as a transition from scale-free to regularity in the complex network's topology.

REFERENCES

ABUGOV, D. I. & OBREZKOV, O. I. 1978 Acoustic noise in turbulent flames. *Combust. Explos. Shock Waves* **14** (5), 606–612.

ALBERT, R., JEONG, H. & BARABASI, A. L. 2000 Error and attack tolerance of complex networks. *Nature* **406** (6794), 378–382.

ALM, E. & ARKIN, A. P. 2003 Biological networks. *Curr. Opin. Struct. Biol.* **13** (2), 193–202.

ARIANOS, S., BOMPARD, E., CARBONE, A. & XUE, F. 2009 Power grid vulnerability: a complex network approach. *Chaos* **19**, 013119.

BARABASI, A. L. 2011 The network takeover. *Nat. Phys.* **8** (1), 14–16.

BARABÁSI, A. L. & ALBERT, R. 1999 Emergence of scaling in random networks. *Science* **286** (5439), 509–512.

BARABASI, A. L., ALBERT, R. & JEONG, H. 1999 Diameter of the world wide web. *Nature* **401** (9), 130–131.

BARABASI, A. L. & BONABEAU, E. 2003 Scale-free networks. *Sci. Am.* **288** (5), 60–69.

BARABASI, A. L. & OLTVAI, Z. N. 2004 Network biology: understanding the cell's functional organization. *Nat. Rev. Genet.* **5** (2), 101–113.

BASTIAN, M., HEYMANN, S. & JACOMY, M. 2009 Gephi: an open source software for exploring and manipulating networks. In *Proceedings of the 3rd International ICWSM Conference*, pp. 361–362.

BELLIARD, A. 1997 Etude expérimentale de l'émission sonore des flammes turbulentes. PhD Dissertation, Universités d'Aix-Marseille, France.

BRAGG, S. L. 1963 Combustion noise. *J. Inst. Fuel* **36** (1), 12–16.

CHAKRAVARTHY, S. R., SHREENIVASAN, O. J., BOEHM, B., DREIZLER, A. & JANICKA, J. 2007*a* Experimental characterization of onset of acoustic instability in a nonpremixed half-dump combustor. *J. Acoust. Soc. Am.* **122** (1), 120–127.

CHAKRAVARTHY, S. R., SIVAKUMAR, R. & SHREENIVASAN, O. J. 2007*b* Vortex-acoustic lock-on in bluff-body and backward-facing step combustors. *Sadhana* **32** (1–2), 145–154.

CHARAKOPOULOS, A. K., KARAKASIDIS, T. E., PAPANICOLAOU, P. N. & LIAKOPOULOS, A. 2014 The application of complex network time series analysis in turbulent heated jets. *Chaos* **24**, 024408.

CHEN, G., DONG, Z. Y., HILL, D. J., ZHANG, G. H. & HUA, K. Q. 2010 Attack structural vulnerability of power grids: a hybrid approach based on complex networks. *Physica* A **389** (3), 595–603.

CHIU, H. H. & SUMMERFIELD, M. 1974 Theory of combustion noise. *Acta Astronaut.* **1** (7), 967–984.

CLAVIN, P. 2000 Dynamics of combustion fronts in premixed gases: from flames to detonations. *Proc. Combust. Inst.* **28** (1), 569–585.

CLAVIN, P. & SIGGIA, E. D. 1991 Turbulent premixed flames and sound generation. *Combust. Sci. Technol.* **78** (1–3), 147–155.

COATS, C. M. 1996 Coherent structures in combustion. *Prog. Energy Combust. Sci.* **22** (5), 427–509.

DAS, R. K. & PATTANAYAK, S. 1993 Electrical impedance method for flow regime identification in vertical upward gas–liquid two-phase flow. *Meas. Sci. Technol.* **4** (12), 1457–1463.

DAVIS, A., MARSHAK, A., WISCOMBE, W. & CAHALAN, R. 1996 Scale invariance of liquid water distributions in marine stratocumulus. Part I: spectral properties and stationarity issues. *J. Atmos. Sci.* **53** (11), 1538–1558.

DONNER, R. V., ZOU, Y., DONGES, J. F., MARWAN, N. & KURTHS, J. 2010 Recurrence networks – a novel paradigm for nonlinear time series analysis. *New J. Phys.* **12**, 033025.

DOWLING, A. P. & MAHMOUDI, Y. 2015 Combustion noise. *Proc. Combust. Inst.* **35** (1), 65–100.

DOWLING, A. P. & STOW, S. R. 2003 Acoustic analysis of gas turbine combustors. *J. Propul. Power* **19** (5), 751–764.

DUBOS, T., BABIANO, A., PARET, J. & TABELING, P. 2001 Intermittency and coherent structures in the two-dimensional inverse energy cascade: comparing numerical and laboratory experiments. *Phys. Rev.* E **64**, 036302.

FRISCH, U. 1995 *Turbulence: The Legacy of AN Kolmogorov*. Cambridge University Press.

GAO, Z. & JIN, N. 2009 Flow-pattern identification and nonlinear dynamics of gas–liquid two-phase flow in complex networks. *Phys. Rev.* E **79** (6), 066303.

GAO, Z. K., JIN, N. D., WANG, W. X. & LAI, Y. C. 2010 Motif distributions in phase-space networks for characterizing experimental two-phase flow patterns with chaotic features. *Phys. Rev.* E **82** (1), 016210.

GOTODA, H., AMANO, M., MIYANO, T., IKAWA, T., MAKI, K. & TACHIBANA, S. 2012 Characterization of complexities in combustion instability in a lean premixed gas-turbine model combustor. *Chaos* **22**, 043128.

GOTODA, H., NIKIMOTO, H., MIYANO, T. & TACHIBANA, S. 2011 Dynamic properties of combustion instability in a lean premixed gas-turbine combustor. *Chaos* **21**, 013124.

GOTODA, H., SHINODA, Y., KOBAYASHI, M. & OKUNO, Y. 2014 Detection and control of combustion instability based on the concept of dynamical system theory. *Phys. Rev.* E **89**, 022910.

HEGDE, U. G., REUTER, D. & ZINN, B. T. 1988 Sound generation by ducted flames. *AIAA J.* **26** (5), 532–537.

KRAICHNAN, R. H. 1967 Inertial ranges in two-dimensional turbulence. *Phys. Fluids* **10**, 1417–1423.

KUMAR, R. N. 1975 Further experimental results on the structure and acoustics of turbulent jet flames. In *AIAA 2nd Aero-Acoustics Conference*, AIAA 75-523, pp. 24–26.

LACASA, L., LUQUE, B., BALLESTEROS, F., LUQUE, J. & NUNO, J. C. 2008 From time series to complex networks: the visibility graph. *Proc. Natl Acad. Sci. USA* **105** (13), 4972–4975.

LACASA, L., LUQUE, B., LUQUE, J. & NUNO, J. C. 2009 The visibility graph: a new method for estimating the Hurst exponent of fractional Brownian motion. *Eur. Phys. Lett.* **86** (3), 1–5.

LESNE, A. & LAGUËS, M. 2011 *Scale Invariance: From Phase Transitions to Turbulence*. Springer.

LIEUWEN, T. C. 2002 Experimental investigation of limit-cycle oscillations in an unstable gas turbine combustor. *J. Propul. Power* **18** (1), 61–67.

LIU, C., ZHOU, W. X. & YUAN, W. K. 2010 Statistical properties of visibility graph of energy dissipation rates in three-dimensional fully developed turbulence. *Physica* A **389** (13), 2675–2681.

LOVEJOY, S. & SCHERTZER, D. 1986 Scale invariance, symmetries, fractals, and stochastic simulations of atmospheric phenomena. *Bull. Am. Meteorol. Soc.* **67** (1), 21–32.

MURUGESAN, M., NAIR, V. & SUJITH, R. I. 2014 System and method for early detection of onset of instabilities using complex networks, Provisional Patent, Filed on 29 April 2014.

NAIR, V. & SUJITH, R. I. 2013 Identifying homoclinic orbits in the dynamics of intermittent signals through recurrence quantification. *Chaos: Interdiscip. J. Nonlinear Sci.* **23**, 033136.

NAIR, V. & SUJITH, R. I. 2014 Multifractality in combustion noise: predicting an impending instability. *J. Fluid Mech.* **747**, 635–655.

NAIR, V., THAMPI, G., KARUPPASAMY, S., GOPALAN, S. & SUJITH, R. I. 2013 Loss of chaos in combustion noise as a precursor for impending instability. *Intl J. Spray Combust. Diag.* **5**, 273–290.

NAIR, V., THAMPI, G. & SUJITH, R. I. 2014 Intermittency route to thermoacoustic instability in turbulent combustors. *J. Fluid Mech.* **756**, 470–487.

NI, X. H., JIANG, Z. Q. & ZHOU, W. X. 2009 Degree distributions of the visibility graphs mapped from fractional Brownian motions and multifractal random walks. *Phys. Lett.* A **373** (42), 3822–3826.

NOIRAY, N. & SCHUERMANS, B. 2012 Theoretical and experimental investigations on damper performance for suppression of thermoacoustic oscillations. *J. Sound Vib.* **331** (12), 2753–2763.

NUNEZ, A. M., LACASA, L., GOMEZ, J. P. & LUQUE, B. 2012 Visibility algorithms: a short review. In *New Frontiers in Graph Theory* (ed. Y. Zhang), pp. 119–152. InTech,; doi:10.5772/34810.

PAGANI, G. A. & AIELLO, M. 2014 Power grid complex network evolutions for the smart grid. *Physica* A **396**, 248–266.

PARET, J. & TABELING, P. 1998 Intermittency in the two-dimensional inverse cascade of energy: experimental observations. *Phys. Fluids* **10** (12), 3126–3136.

POCHEAU, A. 1994 Scale invariance in turbulent front propagation. *Phys. Rev.* E **49** (2), 1109–1122.

POINSOT, T. J., TROUVE, A. C., VEYNANTE, D. P., CANDEL, S. M. & ESPOSITO, E. J. 1987 Vortex-driven acoustically coupled combustion instabilities. *J. Fluid Mech.* **177**, 265–292.

QUENELL, G. 1994 Spectral diameter estimates for *k*-regular. *Adv. Maths* **106** (1), 122–148.

RAJARAM, R. 2007 Characteristics of sound radiation from turbulent premixed flames, PhD thesis, Georgia Institute of Technology, USA.

RAJARAM, R. & LIEUWEN, T. 2009 Acoustic radiation from turbulent premixed flames. *J. Fluid Mech.* **637**, 357–385.

RAYLEIGH, J. W. S. 1878 The explanation of certain acoustical phenomena. *Nature* **18**, 319–321.

ROGERS, D. E. 1956 A mechanism for high-frequency oscillation in ramjet combustors and afterburners. *J. Jet Propul.* **26** (6), 456–462.

ROUHANI, S. Z. & SOHAL, M. S. 1983 Two-phase flow patterns: a review of research results. *Prog. Nucl. Energy* **11** (3), 219–259.

SCHADOW, K. C. & GUTMARK, E. 1992 Combustion instability related to vortex shedding in dump combustors and their passive control. *Prog. Energy Combust. Sci.* **18** (2), 117–132.

SCHADOW, K. C., GUTMARK, E., PARR, T. P., PARR, D. M., WILSON, K. J. & CRUMP, J. E. 1989 Large-scale coherent structures as drivers of combustion instability. *Combust. Sci. Technol.* **64** (4–6), 167–186.

SHATS, M. G., XIA, H. & PUNZMANN, H. 2005 Spectral condensation of turbulence in plasmas and fluids and its role in low-to-high phase transitions in toroidal plasma. *Phys. Rev.* E **71**, 046409.

SMITH, D. A. & ZUKOSKI, E. E. 1985 Combustion instability sustained by unsteady vortex combustion. In *AIAA/SAE/ASME/ASEE 21st Joint Propulsion Conference*, AIAA-85-1248.

SOMMERIA, J. 1986 Experimental study of the two-dimensional inverse energy cascade in a square box. *J. Fluid Mech.* **170**, 139–168.

STRAHLE, W. C. 1971 On combustion generated noise. *J. Fluid Mech.* **49** (02), 399–414.

STRAHLE, W. C. 1978 Combustion noise. *Prog. Energy Combust. Sci.* **4** (3), 157–176.

STROZZI, F., ZALDÍVAR, J. M., POLJANSEK, K., BONO, F. & GUTIÉRREZ, E. 2009 *From Complex Networks to Time Series Analysis and Vice versa: Application to Metabolic Networks*. Office for Official Publications of the European Communities.

WATTS, D. J. & STROGATZ, S. H. 1998 Collective dynamics of 'small-world' networks. *Nature* **393** (6684), 440–442.

XIAO, Z., WAN, M., CHEN, S. & EYINK, G. L. 2009 Physical mechanism of the inverse energy cascade of two-dimensional turbulence: a numerical investigation. *J. Fluid Mech.* **619**, 1–44.

YU, K. H., TROUVE, A. & DAILY, J. W. 1991 Low-frequency pressure oscillations in a model ramjet combustor. *J. Fluid Mech.* **232**, 47–72.

ZANK, G. P. & MATTHAEUS, W. H. 1990 Nearly incompressible hydrodynamics and heat conduction. *Phys. Rev. Lett.* **64** (11), 1243–1246.

ZHANG, J. & SMALL, M. 2006 Complex network from pseudo-periodic time series: topology versus dynamics. *Phys. Rev. Lett.* **96** (23), 238701.